

Thesis ID : IJERTTH0007

General Circulation and Principal Wave Modes in Andaman Sea from Observations



Kiran S R

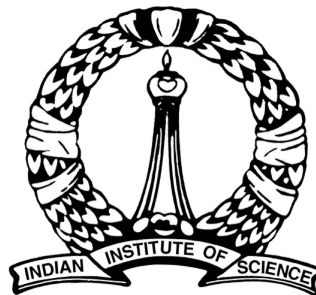
University of Kerala, Kerala
India.

Published By

**International Journal of
Engineering Research and Technology
(www.ijert.org)**

General Circulation and Principal Wave Modes in Andaman Sea from Observations

Research by
KIRAN S R



Centre for Atmospheric and Oceanic Sciences (CAOS)

Indian Institute of Science

Bangalore

INDIA

June 2017



Railay Beach of Thailand, surrounded by Andaman Sea offers a stunning spectacle of natural splendor...



A fuming Barren island...



A busy Strait of Malacca...

“Everything is determined...by forces over which we have no control. It is determined for the insect as well as for the star. Human beings, vegetables, or cosmic dust—we all dance to a mysterious tune, intoned in the distance by an invisible piper.”

— Albert Einstein

Preface

The study "General Circulation and Principal Wave Modes in Andaman Sea from Observations", which was conducted from August 2016 to June 2017, is the realisation of my dream as an independent researcher. It draws insight into the general circulation of Andaman Sea, a strategically important oceanic domain of India, which seldom figured in earlier oceanographic research or expeditions. The discovery of several fluid phenomena in Andaman Sea with the detailed description of each of them makes this study special above all. This research entirely utilised only geophysical data freely available on-line from authentic sources and hence bear no obligation to any other person or institution whatsoever.

I thank my professors P. N. Vinayachandran, Debasis Sengupta, G. S. Bhat, and Jai Sukhatme at Center for Atmospheric and Oceanic Sciences, Indian Institute of Science, with whom I had fruitful discussions and enlightening sessions when I was a Masters student and this propelled me to emerge as an independent researcher. I express my gratitude to my parents and friends, who stood by me through my ups and downs.

Abstract

Objectives: This study intends to describe the Andaman Sea circulation and investigate the dominant modes of variability in the basin.

Analysis/Observations: The domain experiences stronger South-westerly winds from May to September and relatively weaker North-easterlies from November to February. A strong negative Ekman pumping along the north coast of Indonesia is observed during Summer. The transport of water across the straits of Andaman and Nicobar Islands (ANI) is computed by simple mass balance and is found to be in phase with the monthly averaged Mean Sea Level Anomalies (MSLA) of Andaman Sea. There occurs high surface outflux through Great channel and Ten-Degree channel in Summer. In April and October, rate of transport through the straits is maximum. During the same months, meridional surface currents intensify along the eastern boundary of the basin and are associated with signatures of downwelling.

Findings: Intense downwelling occurs to the north coast of Indonesia during Summer, locally forced by south-westerlies. There occurs large influx of water into Andaman Sea between April and November through the straits between the islands. Equatorial Wyrтки jets remotely force Kelvin waves of downwelling nature in the basin during April and October. The circulation in Andaman Sea is characterised by gyres or vortices, which is the manifestation of Rossby waves of semi-annual mode. The basin has a characteristic 120-day mode of westward propagating long Rossby wave packets which reflect from the coast of ANI as eastward propagating short Rossby waves.

Novelty: This is the first attempt to completely describe the dynamics of Andaman Sea circulation exclusively from observations. The landmark discovery of coastal downwelling and upwelling in South Andaman Sea makes this study a special one. Such phenomena have far-reaching consequences on the socio-economic fabric of the country concerned, as this determines the availability of fishes during different times of the year. The discovery of Kelvin Waves and Rossby Wave reflection in Andaman Sea with the detailed description of the wave characteristics is first of its kind in the basin. Hence, this is the first comprehensive study on the dynamics of circulation in Andaman Sea

Keywords: Andaman Sea, Downwelling, Kelvin wave, Rossby wave reflection

Contents

Preface	iv
Abstract	v
Contents	vii
List of Figures	ix
List of Tables	xi
1 Introduction	1
2 Data and Methodology	7
2.1 Data used	7
2.2 Methods adopted	8
3 Analysis, Results and Discussions	9
3.1 Bathymetry and Straits	9
3.2 Winds	10
3.3 Surface Circulation	12
3.4 Transport across Straits	13
3.5 Kelvin Waves	14
3.6 Rossby Wave modes	15
3.6.1 180-day variability	16
3.6.2 120-day variability	17
4 Conclusion	26

Bibliography

28

List of Figures

1.1	The Bay of Bengal	4
1.2	Andaman Islands	5
1.3	Nicobar Islands	6
3.1	Bathymetry (in metres) of A-SEA in 2D and 3D (sectioned along 95E).	17
3.2	Percentage of total area of A-SEA corresponding to different ranges of depth.	18
3.3	Monthly averaged ASCAT winds (in m/s) of A-SEA for the year 2011.	19
3.4	Monthly averaged Ekman Pumping velocity (m/day) for June and December.	20
3.5	Temporal variation of depth of 20 degree isotherm (95 E to 96 E averaged) in metres.	21
3.6	Monthly averaged OSCAR surface currents (cm/s) in January, April, June and October.	21
3.7	Temporal variations of the basin Rainfall, River Influx and Sea Surface Height Anomaly, expressed in volume of water.	22
3.8	Comparison of depth of 20 degree isotherm between eastern and western regions of A-SEA.	22
3.9	Comparison of Morlet wavelet power spectra of Meridional surface currents on the East and West of A-SEA	23
3.10	Morlet wavelet power spectra for AVISO-MSLA.	24
3.11	Longitude-Time plot of 150-230 day bandpass-filtered MSLA.	24
3.12	AVISO-MSLA overlaid with OSCAR currents (150-230 day bandpass-filtered).	25

3.13 Longitude-Time plot of 100-140 day bandpass-filtered MSLA.	25
--	----

List of Tables

3.1	Width of Straits of Andaman and Nicobar Islands.	18
-----	--	----

To my achan and amma...

Chapter 1

Introduction

Extensive research along the warp and the weft of the Indian Ocean, unravelling the mysteries of a legion of oceanic phenomena, were taking place over many decades in the past. Andaman Sea, despite inextricably linked to the Indian Ocean, remained unexplored for a long period of time. It has derived its name from the island group Andaman Islands, which is located in its vicinity. Located to the south of Myanmar, west of Thailand and north of Indonesian Islands, the Andaman Sea is separated from the Bay of Bengal by the Andaman and Nicobar Islands and an associated chain of sea mounts, along the Indo-Burmese Plate boundary. It extends from about 92 E to 100 E, and from 4 N to 20 N (Figure 1.1).

The Andaman and Nicobar Islands are the largest system of archipelago in the Bay of Bengal. Of the 306 islands present, only 38 of them are inhabited; 11 in the Andaman and 13 in the Nicobar island group. This large archipelago is located at a distance of about 1000 km from mainland India. The nearest landmass in the north is Myanmar, roughly 280 km from Landfall Island, the northernmost island in the group. Sumatra is the closest landmass to Great Nicobar in the south, which is located at a distance of 145 km away. From the

economic and commercial point of view, the sea is well known for its abundant structure of coral reefs and incredible diversity of flora and fauna. It has thus taken the role of a tourist destination, although the sea has been traditionally used for fisheries and transportation of goods. Besides, the southern exit of the sea, i.e., the Straits of Malacca, is an integral part of the maritime trade route between Indian Ocean and the Pacific. It is about 805 km wide, narrow stretch of water between Malay Peninsula and Sumatra. The Barren island volcano, the only active volcano in South Asia, stands in the midst of a volcanic belt on the edge of the Indian and Burmese tectonic plates, near Andaman Islands. It is known to have erupted 30 times until 1832 [[Laluraj et.al., 2006](#)]. The lava falling into the sea is forming an island, at an infinitesimal rate, called Hetu Sheth. The political map showing the island groups of Andamans and the Nicobars are given in figures 1.2 and 1.3.

The main source of fresh water into the Andaman Sea is from the river system of Irrawadi, Salween and Thanintharyi. These rivers, which drain into Andaman Sea, have their maximum runoff during the Summer Monsoon [[Varkey et.al., 1996](#), [Wyrcki, 1961](#)]. The sills between the islands, as well as a number of underwater volcanic seamounts, are all potential sources of internal waves [[Osborne and Burch, 1980](#), [Rizal et.al., 2012](#), [Susanto et. al., 2005](#)] in the sea. Internal waves occur within subsurface layers of marine waters that are stratified because of temperature and salinity variations. Disturbances created within the ocean give rise to these waves, which represent a significant mechanism for the transport of momentum and energy within the ocean. Disturbances are often caused by tidal flow passing over shallow underwater obstacles such as a sill or a shallow ridge.

Wyrtki observed that the sea level in Andaman Sea is high during South-West Monsoon due to piling up of water by Ekman drifts [[Wyrtki, 1961](#)], while the sea level plummets during winter. Strong rainy season prevailed in the region from May to November with an annual average rainfall of 2000mm. The domain gets freshened by the influxes from River Irrawady during this period, while from October, water of high salinity gets transported to the north. He has even observed two minima in salinity over the region, over a year. One during the months of September and October due to fresh water influx from rivers and the other due to the flow from the Strait of Malacca during North-East Monsoon. The latter is attributed to the falling sealevel during the period. He further mentioned about strong semi-diurnal tides in Andaman sea.

[Potemra et. al. \[1991\]](#), using ocean models, concluded the flow in the upper ocean layer to be cyclonic in spring and early summer, while it is anti-cyclonic during rest of the year. Strong eastward zonal flows, along the equator in the Indian Ocean (within 2N and 2S), is observed during Boreal Spring (April-May) and Fall (Oct-Nov). These strong jet is called Wyrtki Jet, named after Wyrtki who discovered them in ship drift data [[Nagura et. al., 2005](#), [Wyrtki, 1973](#)]. It is very strong in the upper 100m of ocean. It is primarily driven by the the zonal winds along equator, which produces eastward propagating equatorially trapped Kelvin Wave (of 2nd Baroclinic mode). This wave, upon hitting the west coast of Sumatra, reflects back as Rossby waves and coastal Kelvin waves. The Rossby wave propagates westwards, while the Kelvin wave which is trapped to the coast, moves poleward. [Potemra et. al. \[1991\]](#), in his studies, had shown that the Rossby Waves getting formed in Andaman Sea (A-SEA) are blocked by the Andaman and Nicobar Islands (ANI).

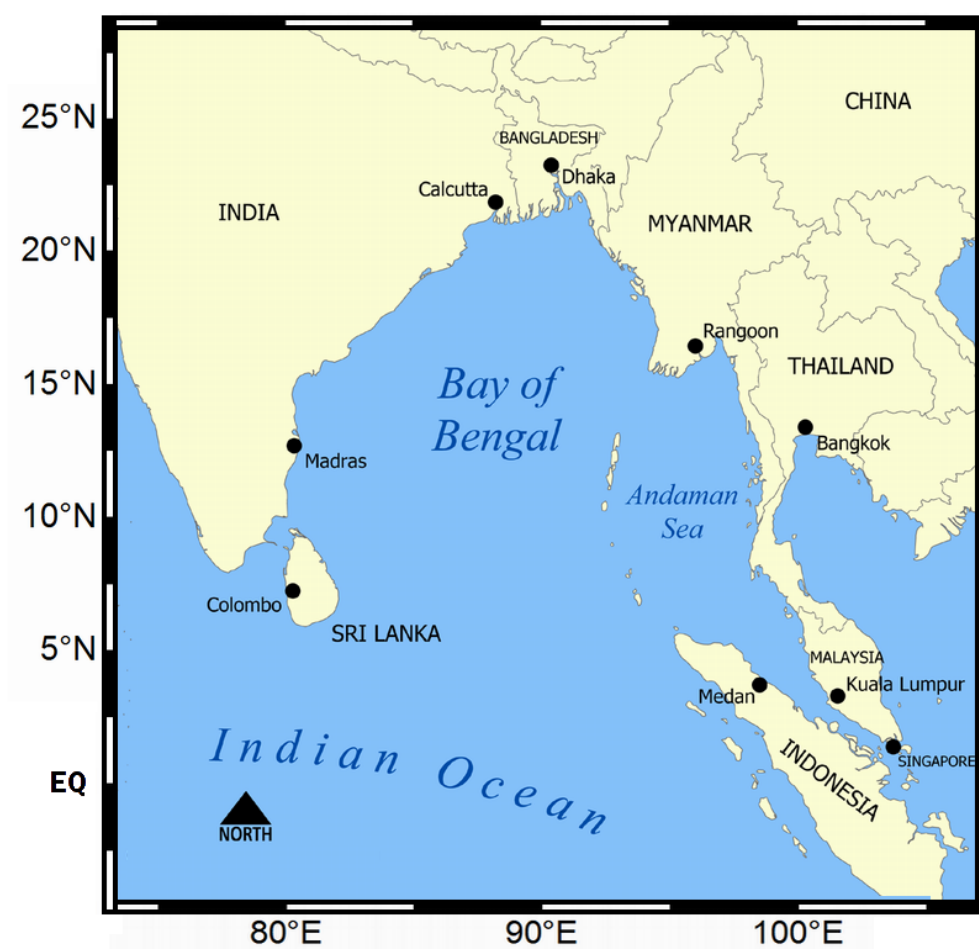


FIGURE 1.1: The Bay of Bengal



FIGURE 1.2. Andaman Islands

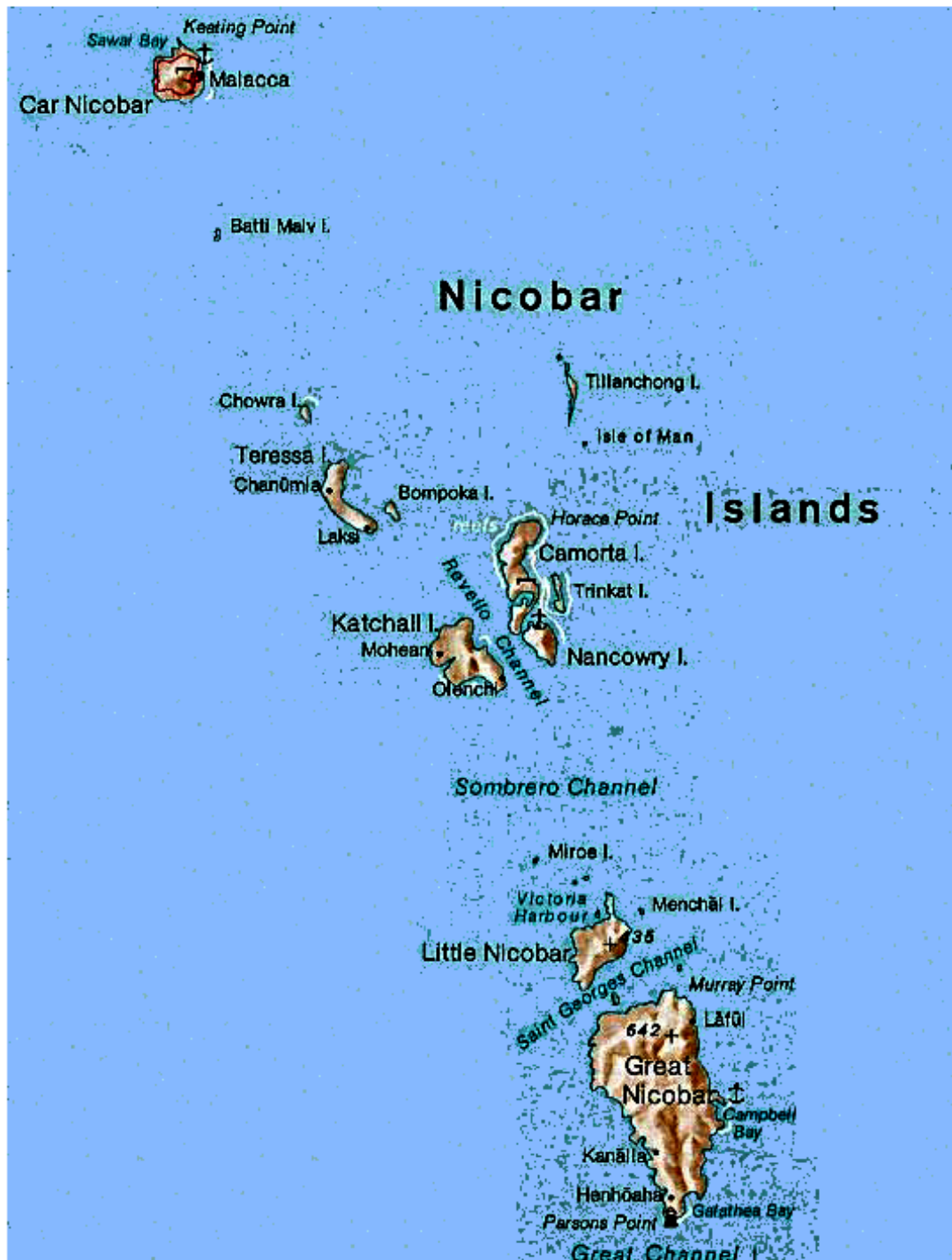


FIGURE 1.3: Nicobar Islands

Chapter 2

Data and Methodology

2.1 Data used

ETOPO5 (5-minute gridded global relief data) is used to study bathymetry of A-SEA. Advanced Scatterometer (ASCAT) data is used to study the surface wind field as well as compute the windstress curl over the region. Monthly averaged climatologies of temperature and salinity with depth are obtained from World Ocean Atlas (WOA) 2013. Sea surface currents are obtained from the Ocean Surface Current Analysis Real-time (OSCAR) estimations with a temporal resolution of 5 days. The Mean Sea Level anomalies (MSLA) altimetry data (with a temporal resolution of 7 days) from Archiving, Validation and Interpretation of Satellite Oceanographic (AVISO) data portal are used to study the ocean circulation and temporal variability of Sea Surface with respect to Mean Sea Level (MSL). Fresh water influx (River Irrawady) into A-SEA is obtained from Global Runoff Data Centre (GRDC)[[Fekete et. al., 2000](#)]. Rainfall data is obtained from Tropical Rainfall Measuring Mission (TRMM).

2.2 Methods adopted

In this study, depth corresponding to 20 degree Celsius isotherm is chosen as the proxy for thermocline depth, the shoaling and deepening of which gives insight into upwelling and downwelling events respectively. The width of the straits between ANI is determined by distance computation method in coordinate geometry, where the geographic coordinates of the north and south coasts of the islands are known. Computation of the curl of wind stress involves spatial derivatives of the wind stress, which is performed by means of simple finite-backward differencing method. To study the dominant modes of variability, techniques such as Wavelet Transforms [[Torrence et. al., 1998](#)] are used to express the geophysical data in both time and frequency domain simultaneously in Figures 3.9 and 3.10. A black solid line scribing the wavelet spectra is the cone of influence, which gives the maximum period upto which the spectrum is significant.

Chapter 3

Analysis, Results and Discussions

3.1 Bathymetry and Straits

The fluid dynamics of an ocean basin is greatly determined by its bathymetry. The first snapshot of Figure 3.1 shows the sea floor relief of A-SEA measured as the depth with respect to mean sea surface level. The northern and eastern side of the basin is shallow, as the continental shelf off the coast of Myanmar and Thailand extends over 200km (marked by 300m isobath). From Figure 3.2, it is evident that about 45 % of the basin area is shallower (less than 500m depth), which is the direct consequence of the presence of the wider shelf. The continental slope which follows the eastern shelf is quite steep between 9N and 14N (see the second snapshot of Figure 3.1). Here, the perspective view of the submarine topography sectioned along 95E exposes the abrupt rise in depth of sea by about 3000m within a short horizontal distance of a degree. Isobaths corresponding to 900m and 2000m are also shown in the figure to emphasize the steepness of the slope. Further, it may be noted that the deep ocean is also not free from sea mounts; hence only around 15% of the total area is deeper than 2500m (Figure 3.2). The western boundary of

A-SEA is marked by volcanic islands and sea mounts, with straits or passages of variable depths that control the entry and exit of water to Bay of Bengal. There occurs a drastic change in depth of water over a small distance of 200km, as one moves from Bay of Bengal (around 3500m deep) to the vicinity of islands (upto 1000m depth) and further into A-SEA. The exchange of water between A-SEA and Bay of Bengal occurs through the straits formed between ANI, the width of which as computed are listed in Table 1. Out of these, the most important straits (in terms of width and depth) are: Preparis Channel (PC), Ten Degree Channel (TDC) and Great Channel (GC), across which major transport shall take place and are indicated in Figure 3.1. PC is the widest but shallowest (250m) of the three and separates South Myanmar from North Andaman. TDC is 600m deep and lies between Little Andaman and Car Nicobar. GC is 1500m deep and separates Great Nicobar from Banda Aceh. These may be considered as the major passages which connect A-SEA to Bay of Bengal and Equatorial Indian Ocean.

3.2 Winds

As observed in Indian Ocean, the wind system over A-SEA regime also reverses every year. The monthly averaged ASCAT winds for 2011 (Figure 3.3) show that the region experiences north-easterlies with an average windspeed of 5 m/s in the months of November to February. During these months, the western part of the domain experiences maximum wind intensity. It weakens by March-April and reverses to strong south-westerlies from May to September, with mean wind speeds touching 8 m/s in June, July and August, distributed

nearly uniform over the entire basin. The wind plummets by October and switch back to north-easterlies from November. The effect of wind stress on ocean surface is explained with the help of wind stress curl. The net divergence of water in the ocean mixed layer results in Ekman Pumping, the vertical velocity of which is given by,

$$W_{ek} = \frac{1}{\rho f} \left[\text{curl}(\Gamma) + \frac{\beta \Gamma_x}{f} \right] \quad (3.1)$$

where Γ is the horizontal windstress in the domain with Γ_x as its zonal component, ρ is the mean density of sea water, $\beta = \frac{\partial f}{\partial y}$ and f is the Coriolis parameter, which is a function of latitude. Here, Γ is obtained from ASCAT windstress and ρ is taken as 1030 kg/m³, and the monthly averaged pumping velocities are evaluated across the basin. Ekman pumping for the months of June and December are shown in Figure 3.4. The comparison between the two seasons elicits a very strong negative pumping velocity of more than 5m/day along the north coast of Indonesia from May to September (shown here, June). This signifies a probable tendency of coastal downwelling in Summers. Besides, it is also observed that the region develops a weak but positive pumping velocity (less than 3m/day) at the mouth of GC in Winters (here, December).

Depth of 20 degree isotherm averaged over the zonal range of 95E to 96E, determined from WOA Temperatures, is shown in Figure 3.5. Generally, the depths are found to be maximum between May and December, and minimum between January and April. There is a definite indication of formation of a cell of strong downwelling to the north of Indonesia, which is marked by the deepening of isotherm (depth exceeding 130m). This originates near the coast in May and spreads further north (upto 9N) during June, July and August. A

strong negative Ekman pumping (discussed in previous paragraph) during the same period suggests the profound impact of local winds in A-SEA during Summer. Shoaling of isotherms occur between January and March, along the entire band of latitudes, although the effect of wind is pronounced more closer to the coast.

3.3 Surface Circulation

OSCAR surface currents for 7 years (2007-2013) are averaged to obtain mean monthly circulation of A-SEA (Figure 3.6). Generally, the currents are found to be stronger at the south than any other part of the basin. An intense surface outflux through GC, of the order of 40cm/s occurs during Summers and Winters. While this flow is directed westwards in Winter, it is southwards along the west coast of Indonesia in Summer. On the other hand, the TDC has strong surface influx in Summer, which weakens by October. This is followed by a sturdy outflux in Winter, which wanes by the month of April. Although the surface flow through PC is generally inward during Summer monsoon, the preceding and succeeding months experience outflow (strong outflow in October, but weak outflow in April). The intense momentum flux through the straits induces strong shear in the flow and thereby resulting in the formation of vortices in the basin, which are either transient and non-periodic, or persistent and periodic. Only the latter is considered for the present study owing to its geophysical relevance. Two gyres, one cyclonic (at the north) and another anticyclonic (at the south), form in A-SEA during May-June and November-December. The circulation changes its polarity during other months, i.e., an anticyclonic vortex and a cyclonic vortex form during August-September and February-March,

at the north and south of the basin respectively (figures not shown here). The circulation is generally weak in January, April, July and October. Hence, the general circulation is characterised by vortices at the north and south of the domain with alternating polarity of semi-annual period. During April and October, when the effects of local winds are minimal, A-SEA experiences the intensification of meridional surface currents in the poleward direction along the continental slope on the eastern side of the basin, with a spatial maxima at 8N, 97E (Figure 3.6). This is characteristic of the propagation of Kelvin Waves, investigations on which are discussed in the Section 3.5.

3.4 Transport across Straits

AVISO-MSLA for 5 years (2005-2009) is spatially averaged to study the monthly variation of Sea Surface Height Anomalies (SSH anomaly) of A-SEA. This is multiplied by the area of the basin to obtain the net volume of water accumulated in the region. It is observed that the water level rises in the basin between April and November (Figure 3.7), with maximum rate of piling up of water during April and October (marked by steep slope of the curve). The rise in SSH is attributed to the following; Rainfall, Fresh water influx from Rivers and inflow of water through the three major straits. Except the last factor, the contributions from Rainfall and Rivers are quantifiable and are hence expressed in volumes of water for comparison (see Figure 3.7). From this, the expected influx through straits ($= \text{SSH anomaly} - \text{Rainfall} - \text{River Influx}$) could be deduced. Here, the evaporative losses are not accounted owing to its diminutive order of magnitude compared to precipitation (Previous studies [[Baumgartner](#)

et. al., 1975] show that the annual mean freshwater gain (precipitation minus evaporation) of A-SEA is 120cm/year). It is found that the SSH of the basin is primarily dictated by the transport of water through the straits. The contributions from Rainfall and Rivers become substantial only during Summers. Hence, a net inward flow occurs through the straits between April and November, followed by net outward transport till March.

3.5 Kelvin Waves

The A-SEA basin experiences very high rate of transport of water through straits in April and October (Figure 3.7). This is a period of equatorial Wyrтки jets[*Wyrtki*, 1973], which hit the coast of Sumatra and reflects back as Rossby Waves and coastal Kelvin Waves. These Kelvin waves are guided along the eastern boundary of Indian Ocean and a part of this signal shall propagate into A-SEA. And the northern coast of Sumatra is the first to sense its effect. Here (within 8N), the 20 degree isotherms are found to deepen during the same period, as observed from Figure 3.5. This is suggestive of the downwelling nature of Kelvin waves. The waves further propagate along the eastern boundary of A-SEA. To confirm this, monthly variations of the depth of 20 degree isotherm for longitudes 94E and 97E (averaged over latitudes 8 N and 13 N) are studied (Figure 3.8). The longitudes are chosen such that one represents the western part of the basin (94E) and the other along the steep continental slope on the eastern side of basin (97E). It is observed that both the longitudes experience deepening of the isotherms in April and October, but the effect is more pronounced at 97E (isotherms deepen by 30m in April and 10m in October). This is a concrete signature of

downwelling in the basin and is definitely not forced locally as the winds are weaker during this period. This confirms unequivocally that the sudden burst of water into the basin through the straits, intensification of eastern boundary currents (see Section 3.3) and the coincidental deepening of isotherms in April and October are the direct consequence of the propagation of downwelling Kelvin waves in A-SEA, remotely forced by equatorial Wyrтки jets. To study the dominant modes of variability, wavelet transform of meridional mean surface currents (7N to 11N averaged) are performed, one on eastern part (95E to 97E averaged) and other along western part of the basin (92E to 94E averaged), as shown in Figures 3.9(a) and 3.9(b) respectively. The eastern region, where the effect of Kelvin waves is pronounced, elicits a strong semi-annual variability (150–230 day), which is totally absent on the western part of the domain. The occurrence of individual events of semi-annual period corresponds to October to December months of 2008, 2011 and 2012. Further, a part of spectral energy on the eastern side of the basin is confined to 40–60 day harmonics, the occurrences of which correspond to March to May months of 2008, 2011, 2012 and 2013. Hence, the Kelvin waves of A-SEA manifest as semi-annual and 40 – 60 day modes of variability.

3.6 Rossby Wave modes

In order to identify the dominant modes of variability in MSLA, wavelet transform of AVISO-MSLA for 20 years (1995-2014) is performed. Figure 3.10 shows the Morlet wavelet power spectra (here, shown only from 2001 to 2006) averaged in space (93E to 97E and 7N

to 12N). Annual (360 day), semi-annual (180 day) and 120-day harmonics are the most dominant modes of variability present in MSLA. The annual mode corresponds to a cycle of rise (during Summer) and fall (during Winter) of SSH per year, controlled by transport across straits (see Section 3.4).

3.6.1 180-day variability

The spectral energy spread over a band of 150-230 days period is filtered for analysis. Figure 3.11 shows the Hovemuller diagram (Longitude-Time plot) of the filtered MSLA for the latitudinal band 7N to 12N. Clear signatures of phase propagation of Rossby Waves with speed $C_p = 5\text{cm/s}$ and $(LxKx/2\pi) = 0.5$ is observed, where Lx and Kx are the length of the basin and wavenumber respectively in the zonal direction. Figure 3.12 shows the evolution of MSLA of the basin, overlaid with OSCAR currents (both 150-230 days Band-passed) from July 2011 to June 2012 (15th of every month). It shows that the domain is composed of vortices; dome-like (and dish-like) structures of high (and low) SSH, with anticyclonic (and cyclonic) circulation around them. These vortices propagate north-westward throughout the year, the northward component of which is rendered by the mean flow. These are characteristic phase propagations of Rossby waves, which manifest as cyclonic and anticyclonic "persistent and periodic" gyres in the general circulation (Section 3.3). Hence, these vortices are not the consequence of intense momentum flux through straits, rather the result of internal perturbations (locally forced by winds and by remotely forced Kelvin waves) propagating as Rossby waves.

3.6.2 120-day variability

Figure 3.13 shows the Hovemuller diagram of the 100-140 day bandpass-filtered MSLA for the latitudinal band 7N to 12N. Definite signatures of Rossby wave reflection is observed here. A wave packet of westward Group velocity ($C_g = 1.3$ cm/s) and westward Phase speed ($C_p = 13$ cm/s) strikes the coasts of ANI and reflect as another wave packet of eastward Group velocity ($C_g = 0.6$ cm/s) and westward Phase speed ($C_p = 6$ cm/s). The incident wave is observed to have longer wavelength $[(LxKx/2\pi) = 0.5]$ than the reflected wave $[(LxKx/2\pi) = 1.5]$, which is the characteristic of Rossby waves.

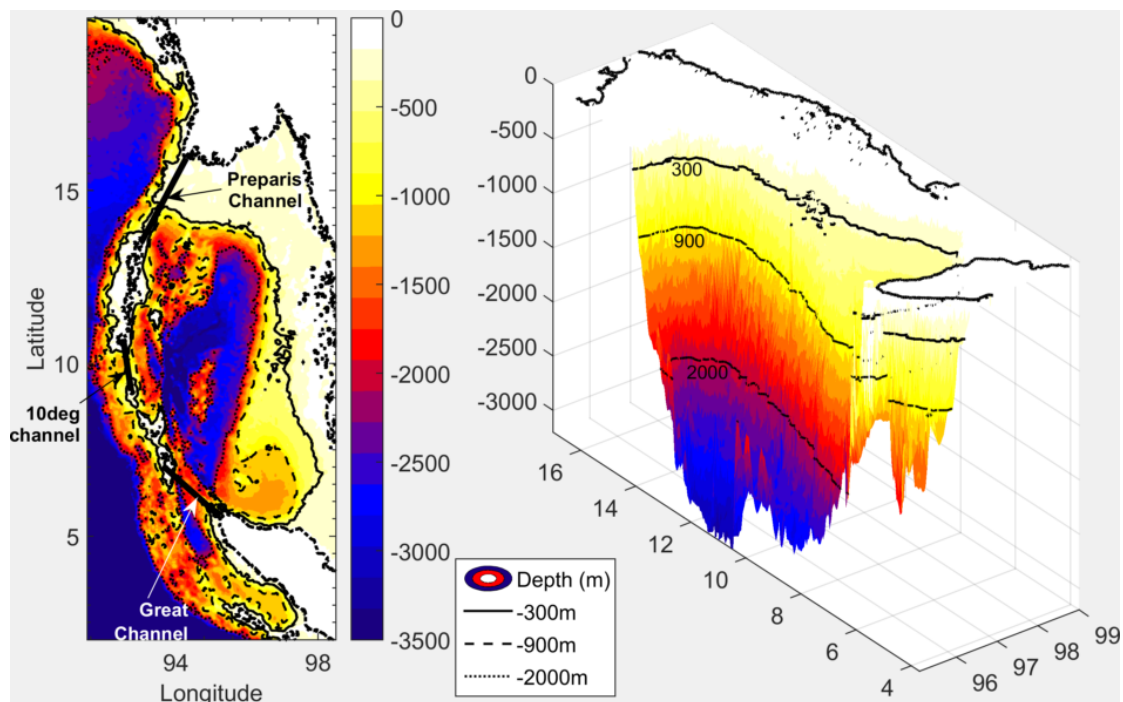


FIGURE 3.1: Bathymetry (in metres) of A-SEA in 2D and 3D (sectioned along 95E).

TABLE 3.1: Width of Straits of Andaman and Nicobar Islands.

Sl.no.	Strait	Distance(km)
1	Preparis Channel	322
2	Mac. Pherson Strait	4
3	Rutland Island - Cinque Island	20
4	Cinque Island - Passage Island	7
5	Passage Island - Sisters Island	8
6	Sisters Island - North Brother Island	18
7	North Brother Island - South Brother Island	8
8	South Brother Island - Little Andaman	8
9	Ten degree Channel	146
10	Car Nicobar - Batti Malv Island	30
11	Batti Malv Island - Chawra Island	47
12	Chawra island - Teressa	13
13	Teressa - Katchal	30
14	Nancowry - Katchal	6
15	Katchal - Little Nicobar (Sombrero Channel)	55
16	Little Nicobar - Great Nicobar (Saint Georges Channel)	18
17	Great Channel	168

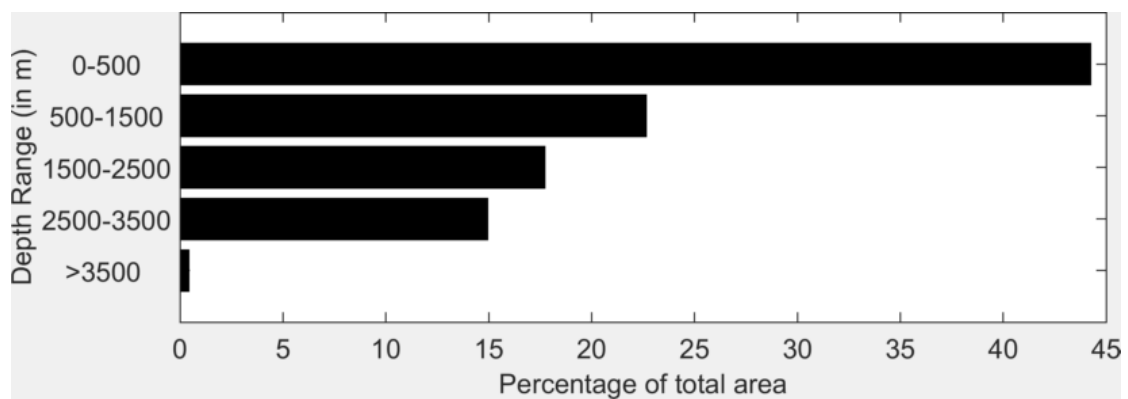


FIGURE 3.2: Percentage of total area of A-SEA corresponding to different ranges of depth.

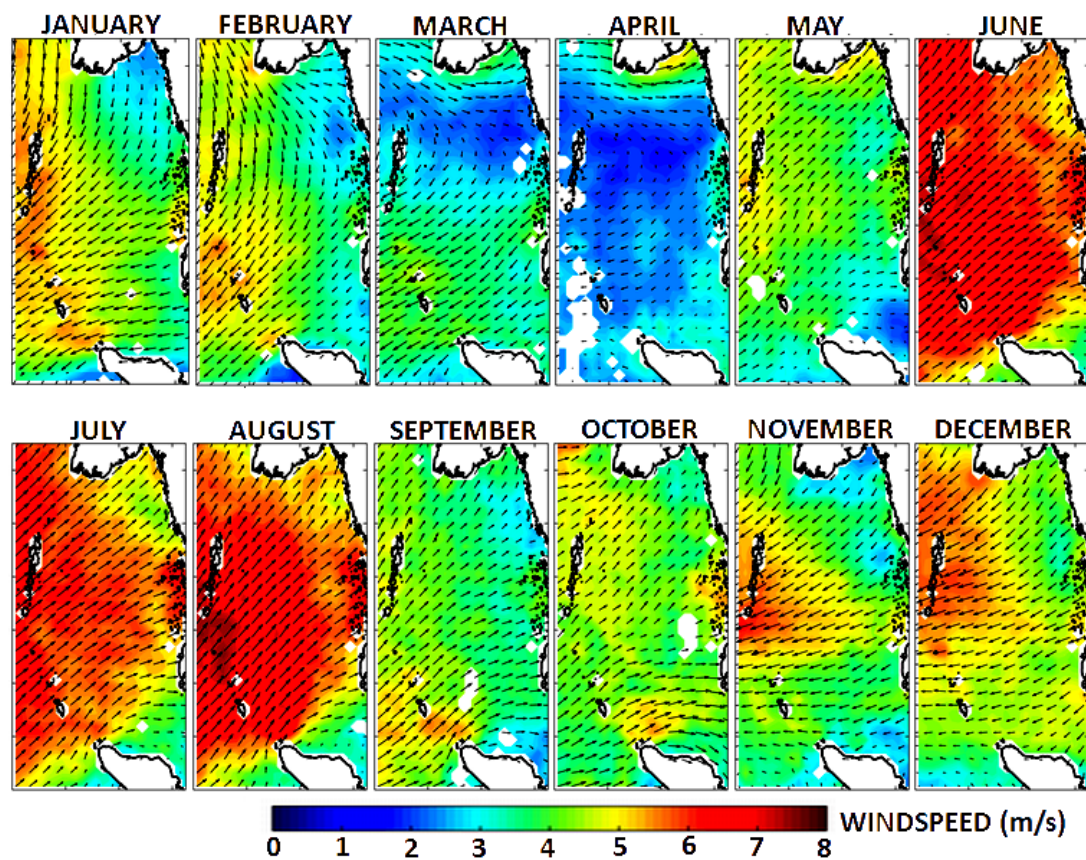


FIGURE 3.3: Monthly averaged ASCAT winds (in m/s) of A-SEA for the year 2011.

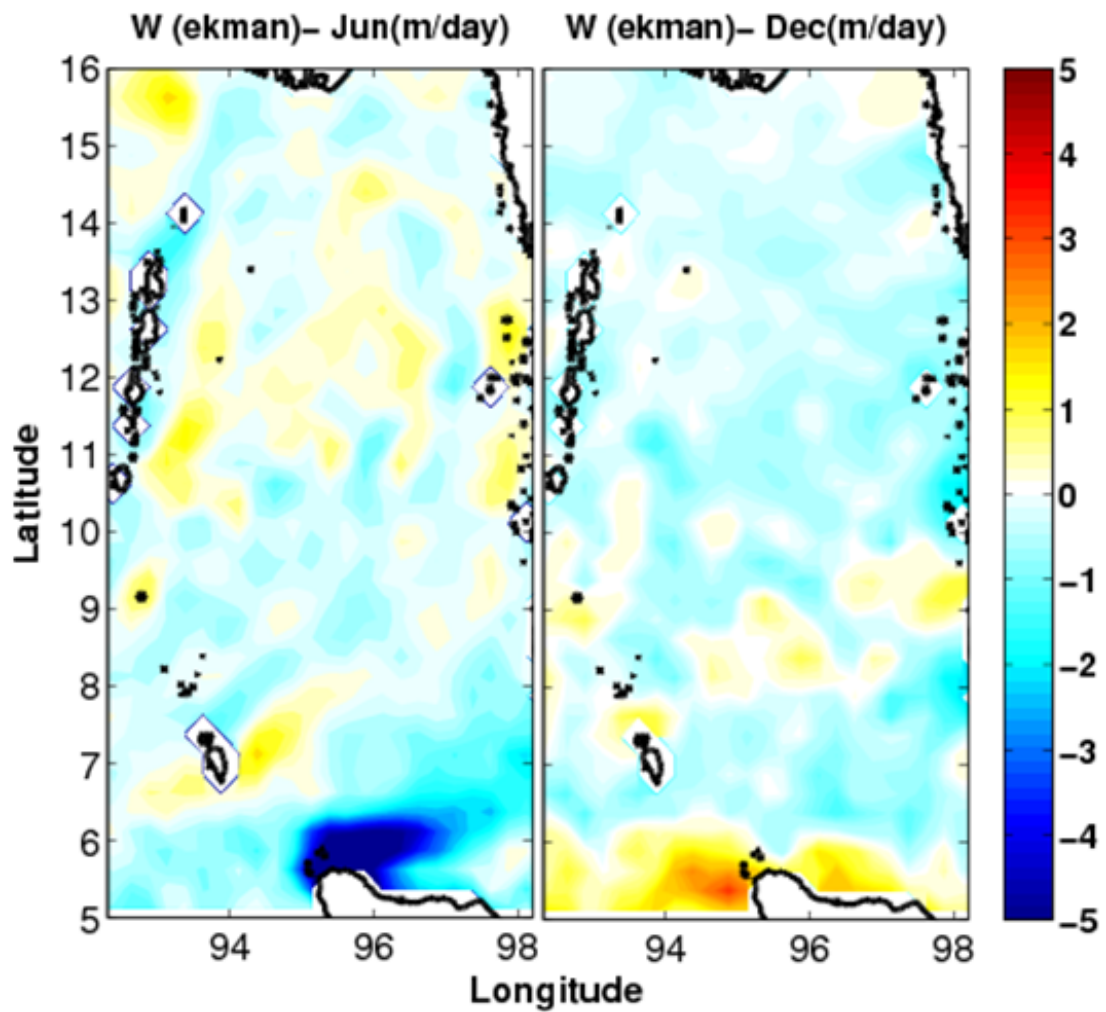


FIGURE 3.4: Monthly averaged Ekman Pumping velocity (m/day) for June and December.

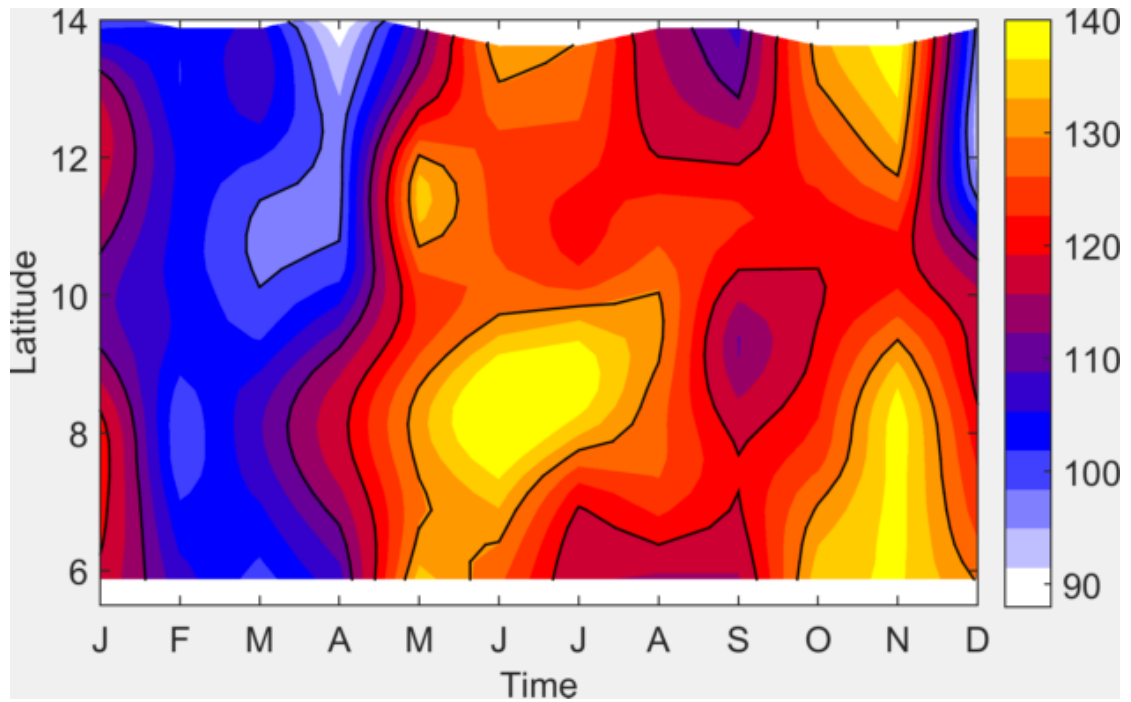


FIGURE 3.5: Temporal variation of depth of 20 degree isotherm (95 E to 96 E averaged) in metres.

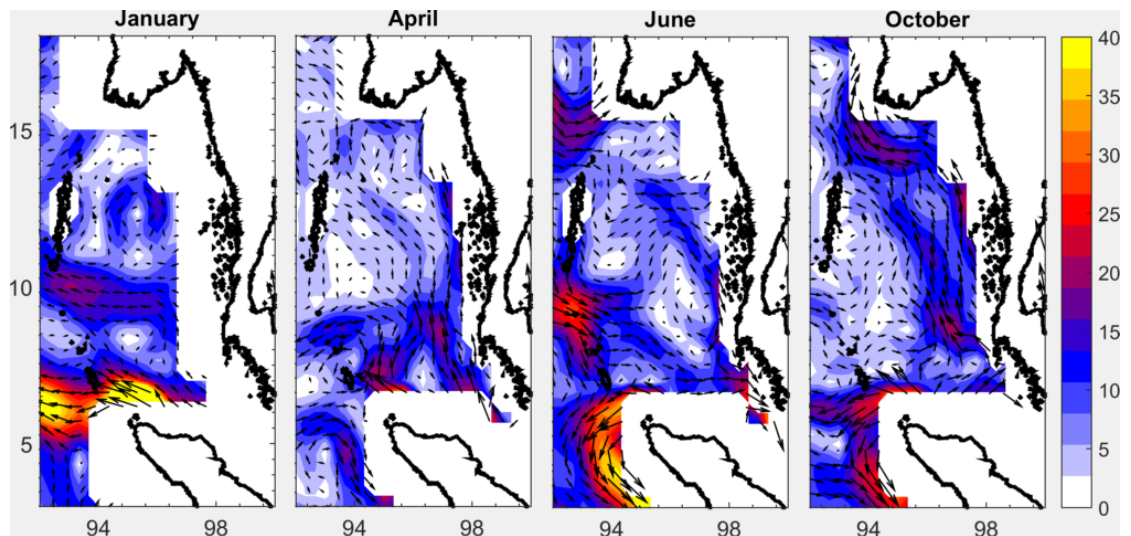


FIGURE 3.6: Monthly averaged OSCAR surface currents (cm/s) in January, April, June and October.

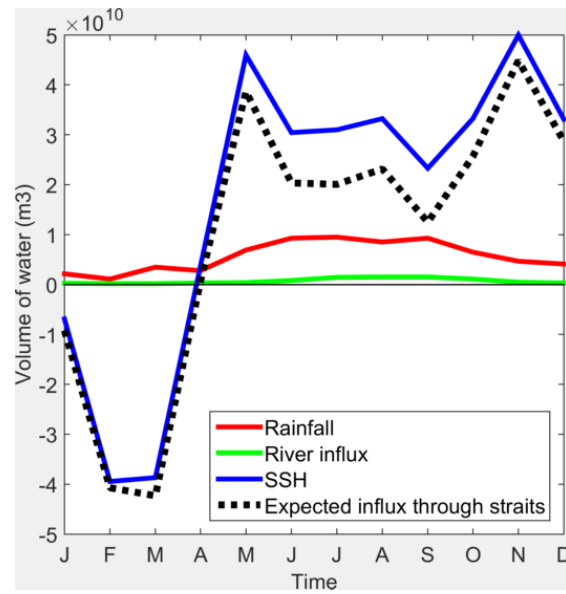


FIGURE 3.7: Temporal variations of the basin Rainfall, River Influx and Sea Surface Height Anomaly, expressed in volume of water.

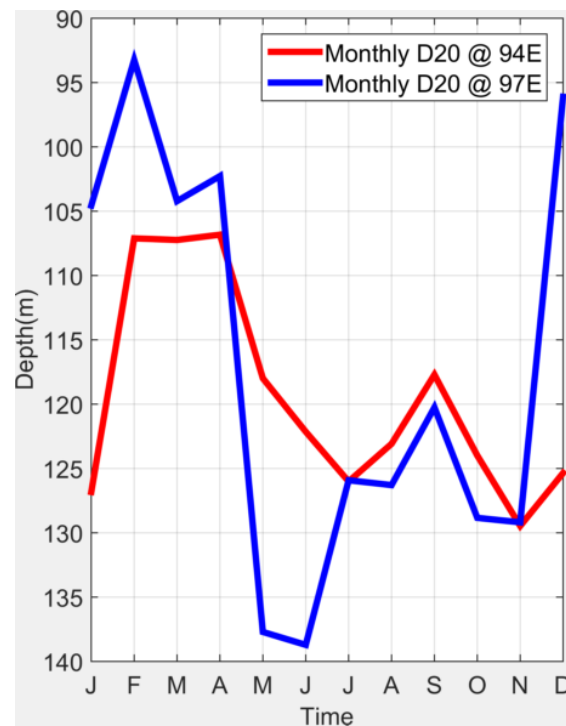
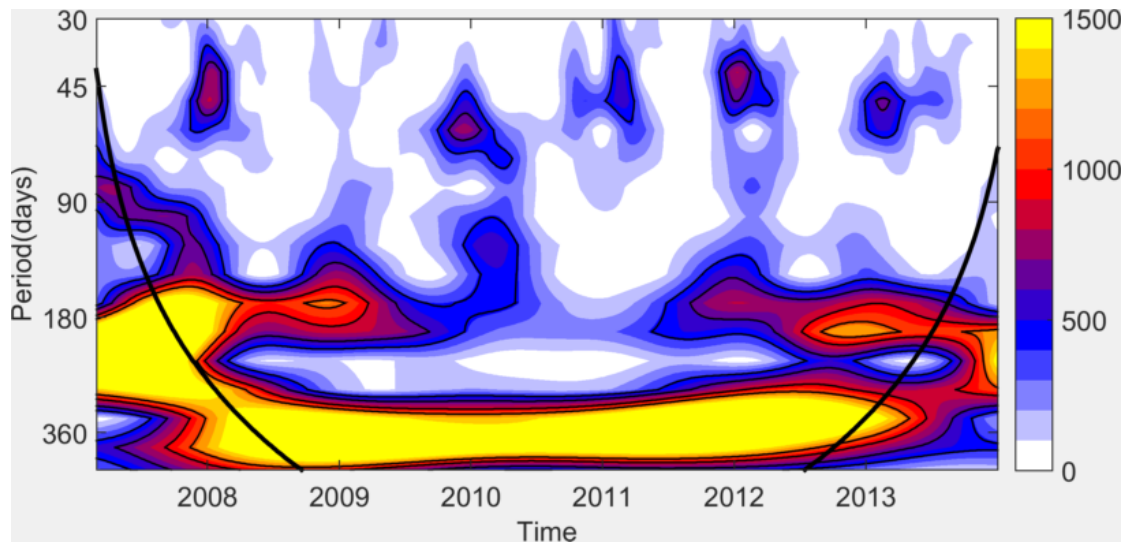
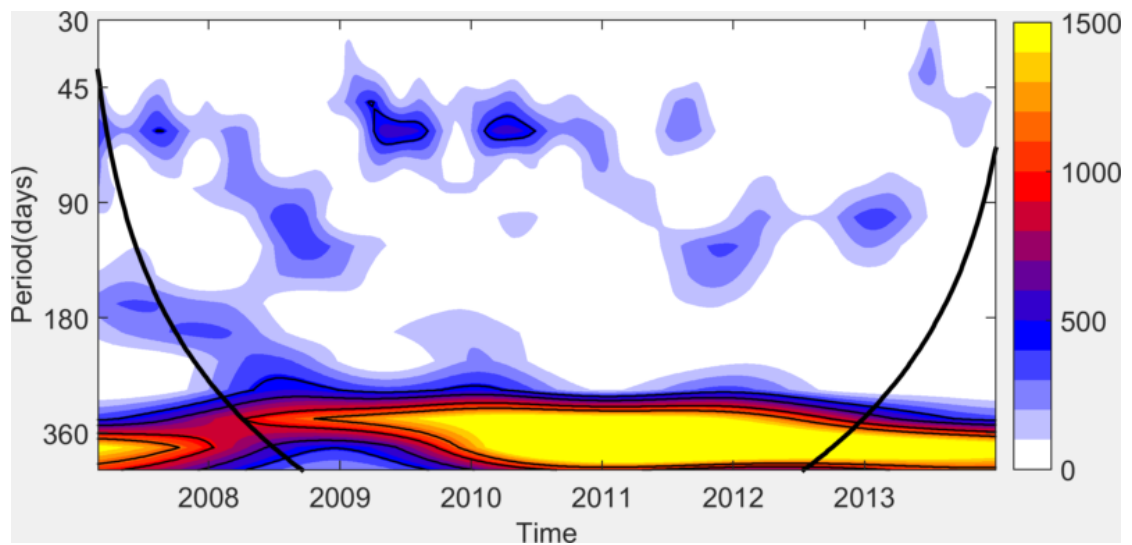


FIGURE 3.8: Comparison of depth of 20 degree isotherm between eastern and western regions of A-SEA.



(a) 95E to 97E zonal averaged



(b) 92E to 94E zonal averaged

FIGURE 3.9: Comparison of Morlet wavelet power spectra of Meridional surface currents on the East and West of A-SEA .

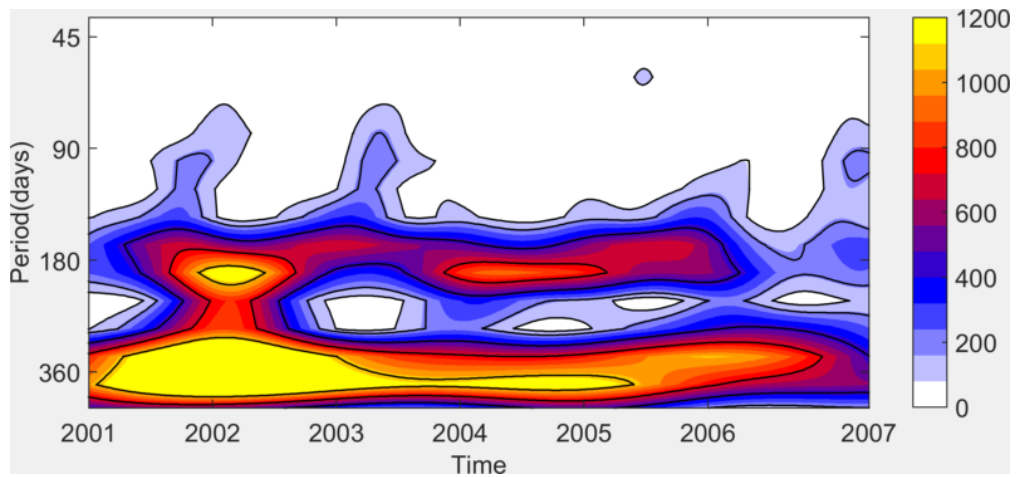


FIGURE 3.10: Morlet wavelet power spectra for AVISO-MSLA.

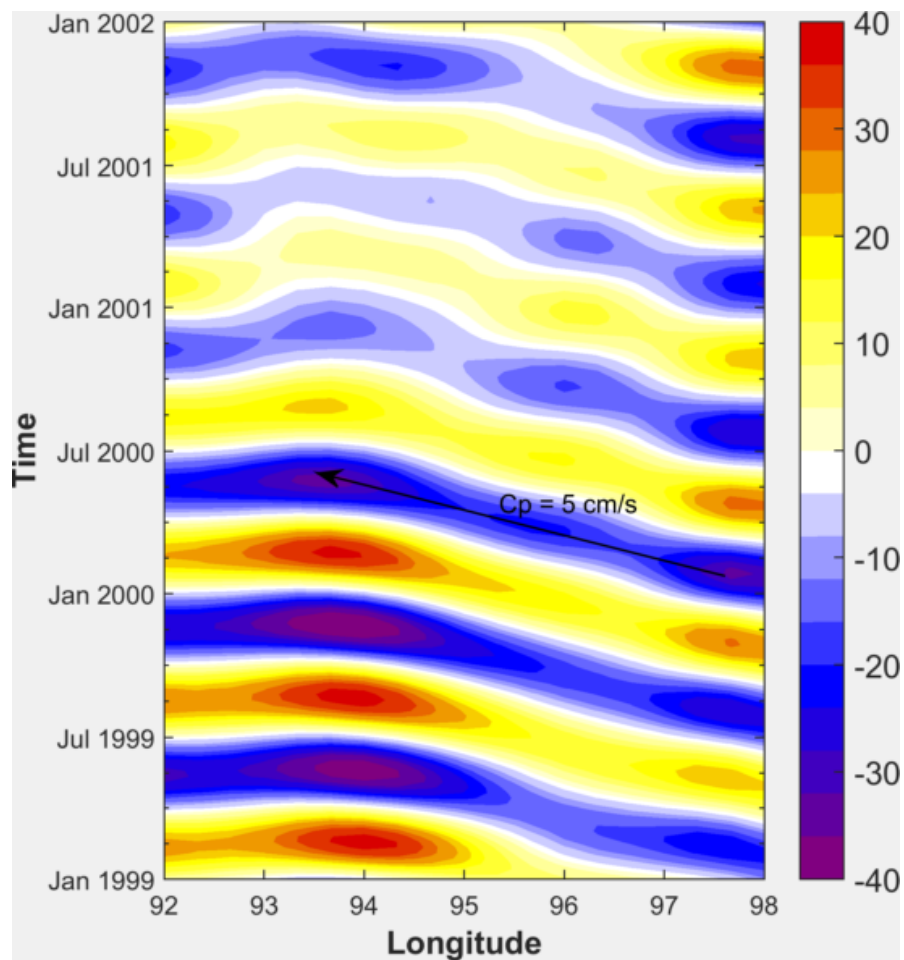


FIGURE 3.11: Longitude-Time plot of 150-230 day bandpass-filtered MSLA.

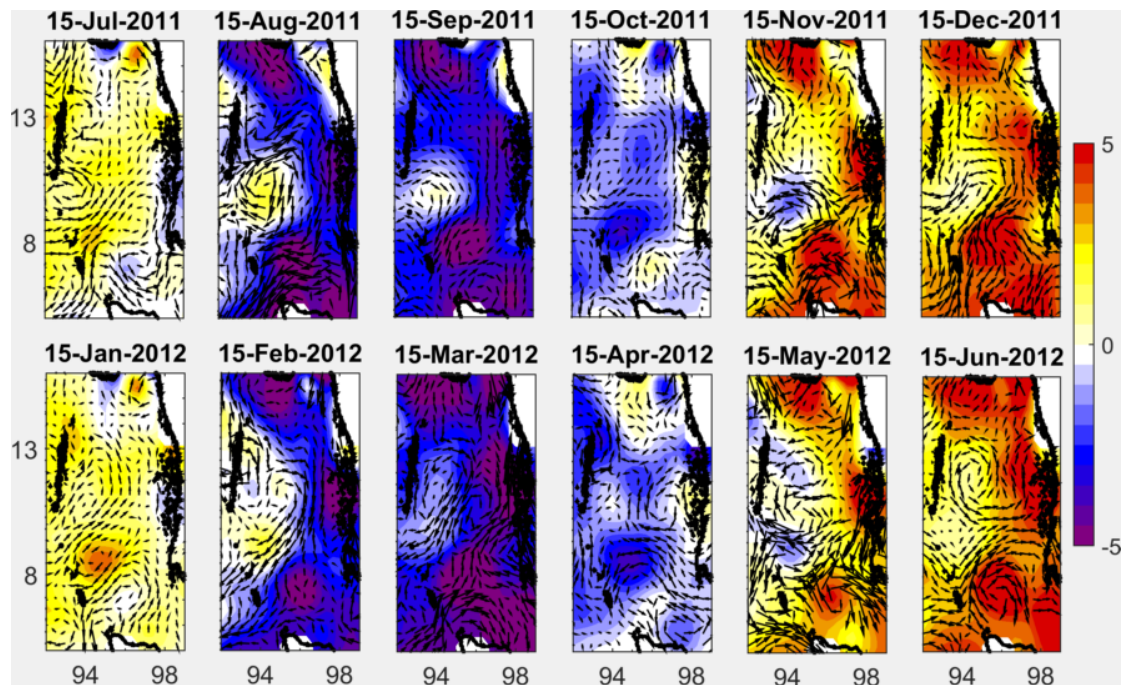


FIGURE 3.12: AVISO-MSLA overlaid with OSCAR currents (150-230 day bandpass-filtered).

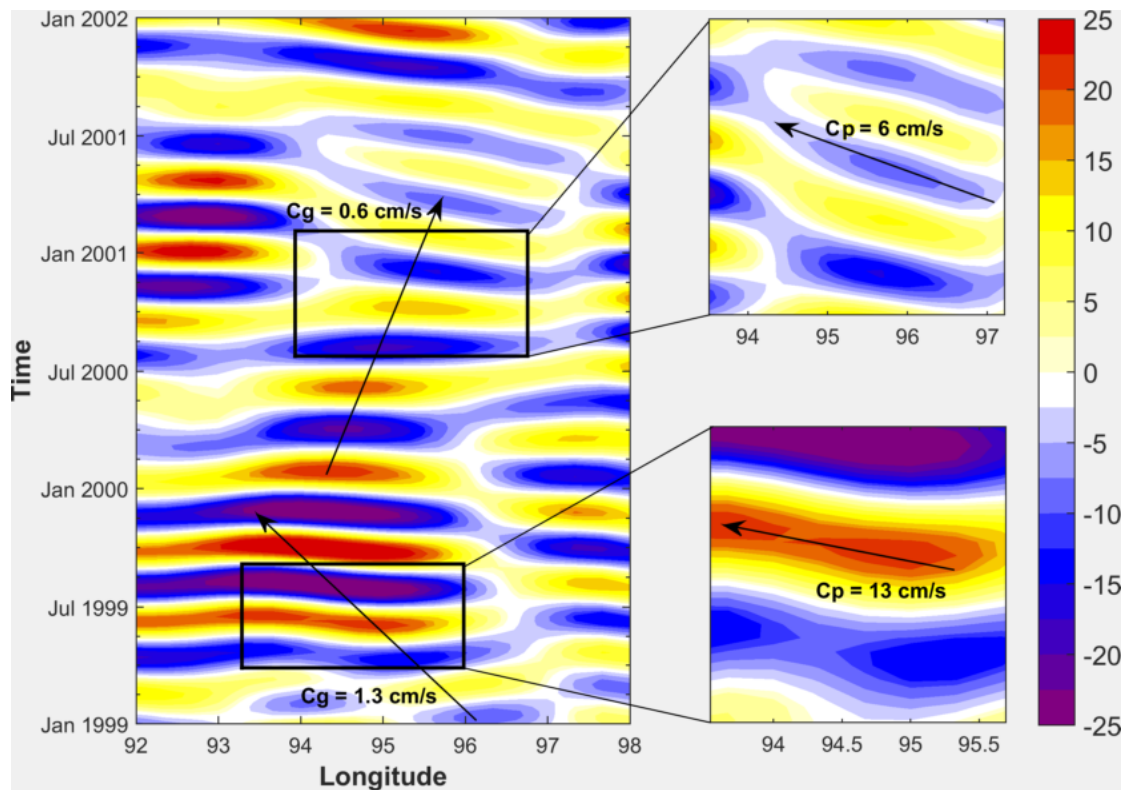


FIGURE 3.13: Longitude-Time plot of 100-140 day bandpass-filtered MSLA.

Chapter 4

Conclusion

This study delves into the dynamics of Andaman Sea circulation with specific insight into dominant wave modes of the basin. The following are the major conclusions arrived at by this study.

- Wind system over Andaman Sea conforms to the general seasonal variability of Indian Ocean. They are strong south-westerlies during Summers (May to September) and relatively weaker north-easterlies during Winters (November to March).
- A cell of strong downwelling forms to the north of Indonesia during Summer. This is accompanied by a high value of negative Ekman pumping velocity over the same region. This means that the effect of local forcing is predominant in Summers.
- Sea Surface Height of Andaman Sea is primarily influenced by the transport across the straits between the islands of Andaman and Nicobar. The flow through the straits is inward from April to November, followed which the flow becomes truly outward from December to March.
- During the months of April and October, coastal Kelvin waves propagate along the eastern boundary of Andaman Sea, remotely

forced by equatorial Wyrtki jets. This is corroborated by intensification of along-shore meridional surface currents, abrupt burst of water into the basin through the straits and the concomitant deepening of 20 degree isotherms. The basin experiences downwelling along its trajectory. The semi-annual and 40-60 day harmonics are the dominant modes of variability associated with the wave.

- Dominant modes of Rossby waves in Andaman Sea are 180-day and 120-day harmonics. Rossby waves of semi-annual period propagate north-westward with phase speed of 5cm/s and are responsible for the vortex formation in the domain. These appear as cyclonic and anticyclonic gyres or circulation with alternating polarity at the north and south of the basin. The 120-day mode manifest as long Rossby waves with westward Group velocity, which strikes the coasts of Andaman and Nicobars and reflects back as short Rossby waves of eastward Group velocity.

Bibliography

Baumgartner A., Riechel E. (1975), The World Water Balance, Mean Annual Global, Continental and Maritime Precipitation, Evaporation and Runoff, *Elsevier*, pp. 1-179.

Fekete B. M., Vorosmarty C. J., Grabs W. (2000), Global Composite Runoff fields based on observed river discharge and simulated water balances, *Global Runoff Data Centre Rep.*, pp. 1-39.

Laluraj C.M., Balachandran K.K, Sabu P. and Saramma (2006), Persistent volcanic signature observed around Barren Island, Andaman sea, India, *Marine Geophysical Researches*, vol.27(4), 283-288p.

Motoki Nagura and Michael J. McPhaden (2010), Wyrтки Jet dynamics: Seasonal variability, *J. Geophysical Research*, 115, 1-17p.

Osborne A.R. and T.L. Burch (1980), Internal solitons in the Andaman sea, *Science*, 208, 451-460p.

Potemra, J. T., Luther, M. E., and Ó Brien, J. J. (1991). The seasonal circulation of the upper ocean in the Bay of Bengal, *Journal of Geophysical Research*, 96, 12667-12683p.

Syamzul Rizal, Peter Damm, Jurgen Sundermann and Muhammad (2012), General Circulation in the Malacca Strait and Andaman sea: A Numerical model study, *American Journal of Environmental Science*, 8(5), 479-488p.

- Susanto R.D., L. Mitnik and Q. Zheng (2005), Ocean internal waves observed in Lombok strait, *Oceanography*, 18, 80-87p.
- Torrence, the Christopher and Compo, G. P., 1998, A practical guide to Wavelet Analysis, *Bulletin of the American Meteorological Society*, 79, 61-78pp.
- Wyrtki, K. (1973), An equatorial jet in the Indian Ocean, *Science*, 181, 262–264p.
- Varkey M.J., Murty V.N.S. and Suryanarayana A. (1996), Physical oceanography of the Bay of Bengal and Andaman sea, *Oceanography and Marine Biology: an Annual Review*, 34, 1-70p.
- Venkatesan, R., V. R. Shamji, G. Latha, R. R. Rao, Arul Muthiah and M. A. Athmanand (2013), Insitu Ocean subsurface timeseries measurements from OMNI buoy network in the Bay of Bengal, *Current Science*, 104, 1166–1177p
- Wyrtki, K. 1961, Physical Oceanography of Southeast Asian waters, *University of California*, 1st Edition, pp: 195.